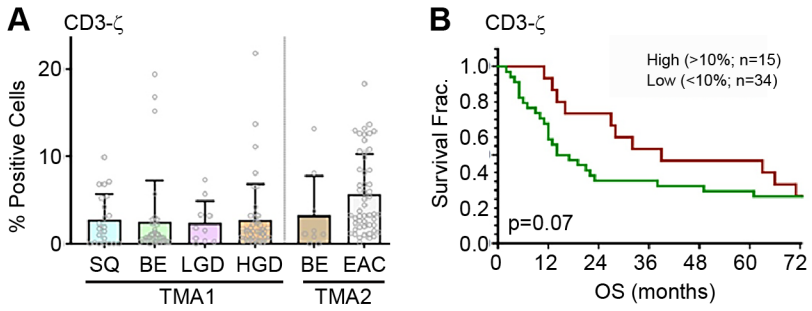

Supplemental Figure 1. CD3ζ expression increases during progression from BE to EAC, with only minimal effects on patient OS. (A) BE, LGD, HGD, or EAC tissue was incorporated into a TMA and stained for CD3ζ. Positive cells per core were counted ad expressed as a percentage of the total cell number. (**B)** Survival analysis shows no significant effects of CD3ζ high vs. low expressing cell on overall patient survival. Survival curves differences were determined using Mantel-Cox regression analysis.

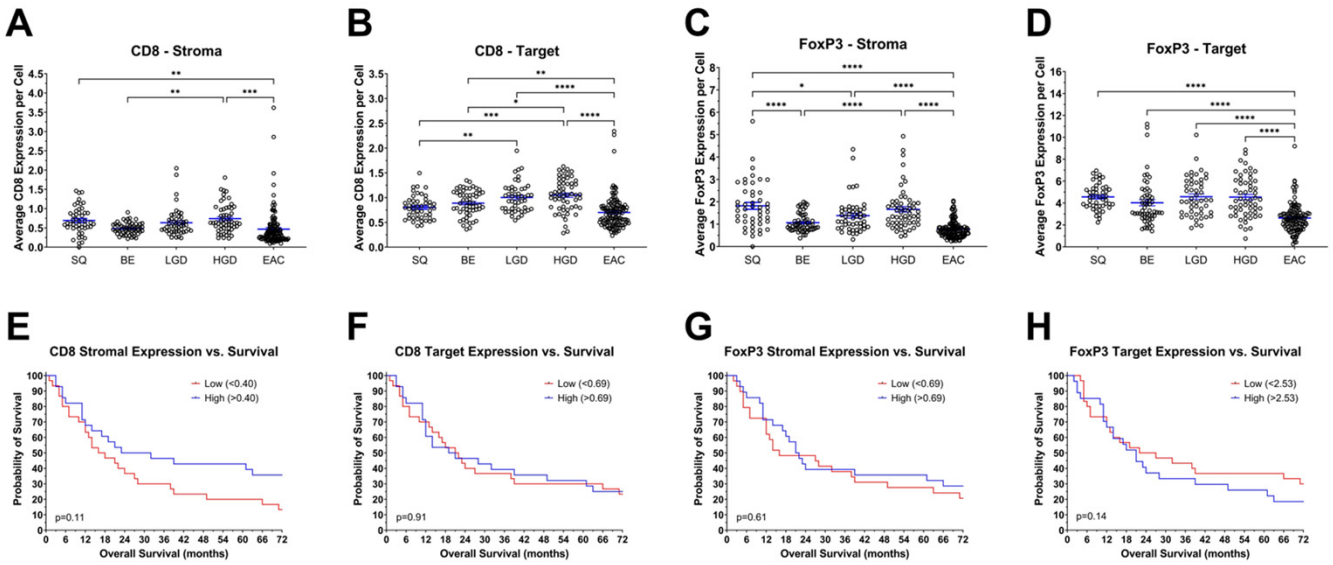

Supplemental Figure 2. Effector and Regulatory T-cell populations changes during progression from BE to EAC and their effects on overall patient survival. A-B, Effector T-cell populations were identified as $CD8^+$ cell populations and the average expression per cell was determined using the Akoya InForm software. Target tissue was identified as CK^+ tissue. $CD8^+$ T-cell populations increase incrementally during progression from BE to HGD in Stroma (A) and Target (B) tissue, respectively. However, EAC tissues are immune poor for effector T-cells. **C-D,** Similarly, FoxP3 expression in T-regulatory cells increase during progression from BE to HGD. However, EAC tissues show low levels of FoxP3+ T-cell populations in either Stroma (C) or Target (D) tissues, respectively. **E-H,** Survival analysis shows no significant effects of either $CD8^+$ high vs. low expressing cell populations or FoxP3+ high vs. low expression cell populations on overall patient survival. Survival curves differences were determined using Mantel-Cox regression analysis.

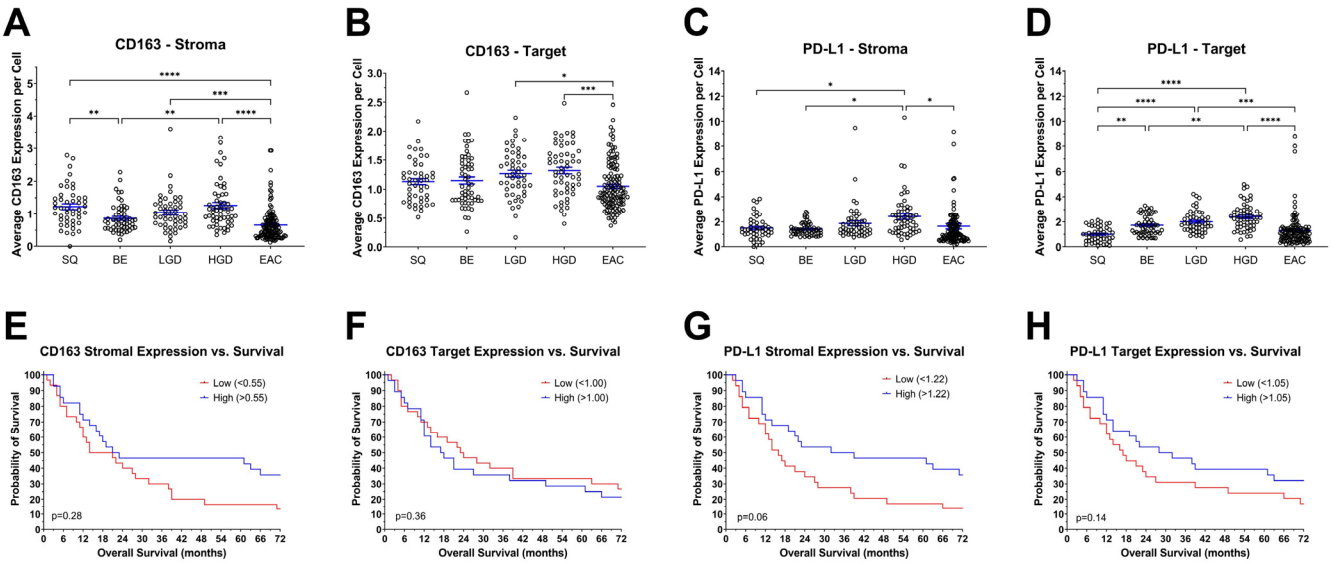

Supplemental Figure 3. Antigen-presenting cell populations change during progression from BE to EAC and their effects on overall patient survival. (A-B) Macrophages were identified as CD163$^+$ cell populations and the average expression per cell was determined using the Akoya InForm software. Target tissue was identified as CK$^+$ tissue. CD163$^+$ macrophages increase incrementally during progression from BE to HGD in Stroma (A) and Target (B) tissue, respectively. However, EAC tissues are immune poor for macrophages. **(C-D)** Similarly, PD-L1 expression in APCs increases during progression from BE to HGD. However, EAC tissues show low levels of PD-L1$^+$ APCs in either Stroma (C) or Target (D) tissues, respectively. **(E-H)** Survival analysis shows no significant effects of either CD163$^+$ high vs. low expressing cell populations or PD-L1+ high vs. low expression cell populations on overall patient survival. Survival curves differences were determined using Mantel-Cox regression analysis.

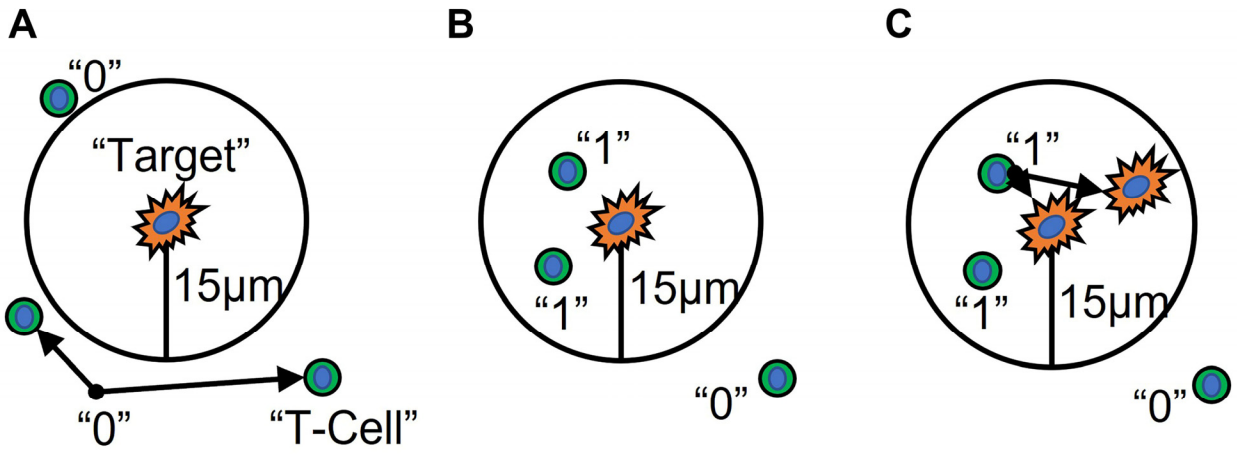

Supplemental Figure 4. Cell Engagement Analysis for T-Cell engagement with epithelium or APCs. (A-C) Multiplex stained images were analyzed using Akoya InForm cell analysis software. Cartoon representation of engagement analysis. PanCK+ epithelial cells, CD163+ macrophages, or PD-L1+ APCs were identified by positive staining as target cells. From each positive target cell, the analysis software determined whether CD3+, CD8+, or FoxP3+ T-cells were within a 15µm radius of the target cell and considered "engaged". A cell outside the radius was given a "0" value as a non-engaged cell (A). Any T-cell within the 15µm radius was given a value of "1" and scored as "engaged" (B). This scoring system prevented T-cells from being counted multiple times, as shown in (C).

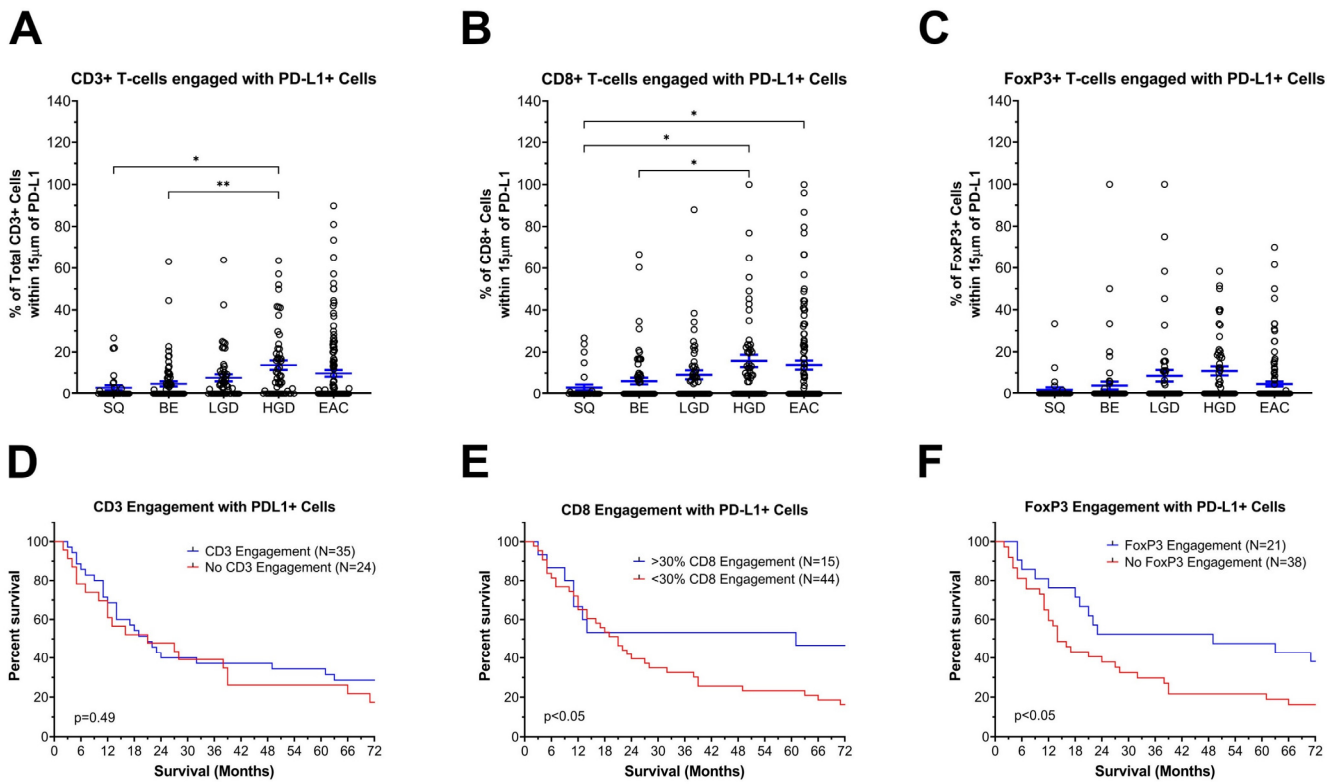

Supplemental Figure 5. T-cell engagement with PD-L1+ APCs minimally affects patient OS. (A) CD3+ T-cells within 15µm of a PD-L1+ APC were counted as "engaged" with the epithelium. The percentage of engaged cells was determined by dividing the number of CD3+ engaged cells by the total number of CD3+ T-cells and multiplying by 100. T-cell engagement increased during progression from BE to HGD. However, CD3+ T-cell engagement within EAC tissue decreased compared to HGD. (**B)** CD8+ effector T-cells within 15µm of a PD-L1+ APC were counted as "engaged" with the epithelium. The percentage of engaged cells was determined by dividing the number of CD8+ engaged cells by the total number of CD8+ T-cells and multiplying by 100. Effector T-cell engagement increased during progression from BE to HGD. However, CD8+ T-cell engagement within EAC tissue decreased compared to HGD. **(C)** FoxP3+ T-regulatory cells within 15µm of a PD-L1+ APC were counted as "engaged" with the epithelium. The percentage of engaged cells was determined by dividing the number of FoxP3+ engaged cells by the total number of FoxP3+ T-cells and multiplying by 100. T-regulatory cell engagement increased during progression from BE to HGD. However, FoxP3+ T-regulatory cell engagement within EAC tissue decreased compared to HGD. (**D-F)** Survival analysis shows no significant effects of $CD3^+$ **(D)** on OS. However, high $CD8^+$ **(E)**, or $FoxP3^+$ **(F)** high engaged tissues had marginally better overall patient survival compared to low engaged tissues. Survival curves differences were determined using Mantel-Cox regression analysis.

```
Sequence 1: Zeta         164 aa
Sequence 2: Delta        171 aa
Sequence 3: Epsilon      207 aa
Sequence 4: Gamma        182 aa

Sequences (1:2) Aligned. Score: 11.5854
Sequences (1:3) Aligned. Score: 11.5854
Sequences (1:4) Aligned. Score: 14.0244
Sequences (2:3) Aligned. Score: 15.2047
Sequences (2:4) Aligned. Score: 36.2573
Sequences (3:4) Aligned. Score: 15.3846


Delta           ---MEHSTFLSGLVLATLLSQVSP---------FKIPIEELEDRVFVNCN----TSITWV
Gamma           ---MEQGKGLAVLILAIILLQGTLAQSIKGNHLVKVYDYQEDGSVLLTCDAE-AKNITWF
Epsilon         MQSGTHWRVLGLCLLSVGVWGQDGNEEMGGITQTPYKVSISGTTVILTCPQYPGSEILWQ
Zeta            -------MKWKALFTAAILQAQLP----------ITEAQSFGLLDPKLCYLL--DGILFI
                             . :  :                              *       * :

Delta           EG--TVGTLLSDITRLDLG-------KRILDPRGIYRCNGTDIY-KDKESTVQVHYRMCQ
Gamma           KDGKMIGFLTEDKKKWNLG-------SNAKDPRGMYQCKGS----QNKSKPLQVYYRMCQ
Epsilon         HNDKNIGGDEDDKNIGSDEDHLSLKEFSELEQSGYYVCYPRGSKPEDANFYLYLRARVCE
Zeta            YGVILTALFLRVKFSRSAD--------APAYQQGQNQLYNELNLGRREEYDVLDKRRGRD
                 .    .         .                *           .  .  :    *  :

Delta           SCVELDPATVAGIIVTDVIATLLLALGVFCFAGH------------ETGRLSGAADTQA
Gamma           NCIELNAATISGFLFAEIVSIFVLAVGVYFIAGQ------------DGVRQSRASDKQT
Delta           LLRNDQVYQPLRDRDDAQYSHLGGNWARNK'WSKNRKAKAKPVTRGAGAGGRQRGQNKERP
Gamma           LLPNDQLYQPLKDREDDQYSHLQGNQLRRN'SEIG------------------MKGERRR
Epsilon         PPVPNPDYEPIRKGQRDLYSGLNQRRI---                        . :
Zeta            GKGHDGLYQGLSTATKDTYDALHMQALPPR
                    :  *: :       *. *  .
```

Supplemental Figure 6. Pairwise amino acid sequence alignments between different CD3 isoforms (ε, δ, γ, ζ) performed using CLASTALW multiple sequence alignment tool. Top panel includes alignment score showing CD3-δ and CD3-γ with highest alignment score of ~36%. '*' indicates that the residues are identical.

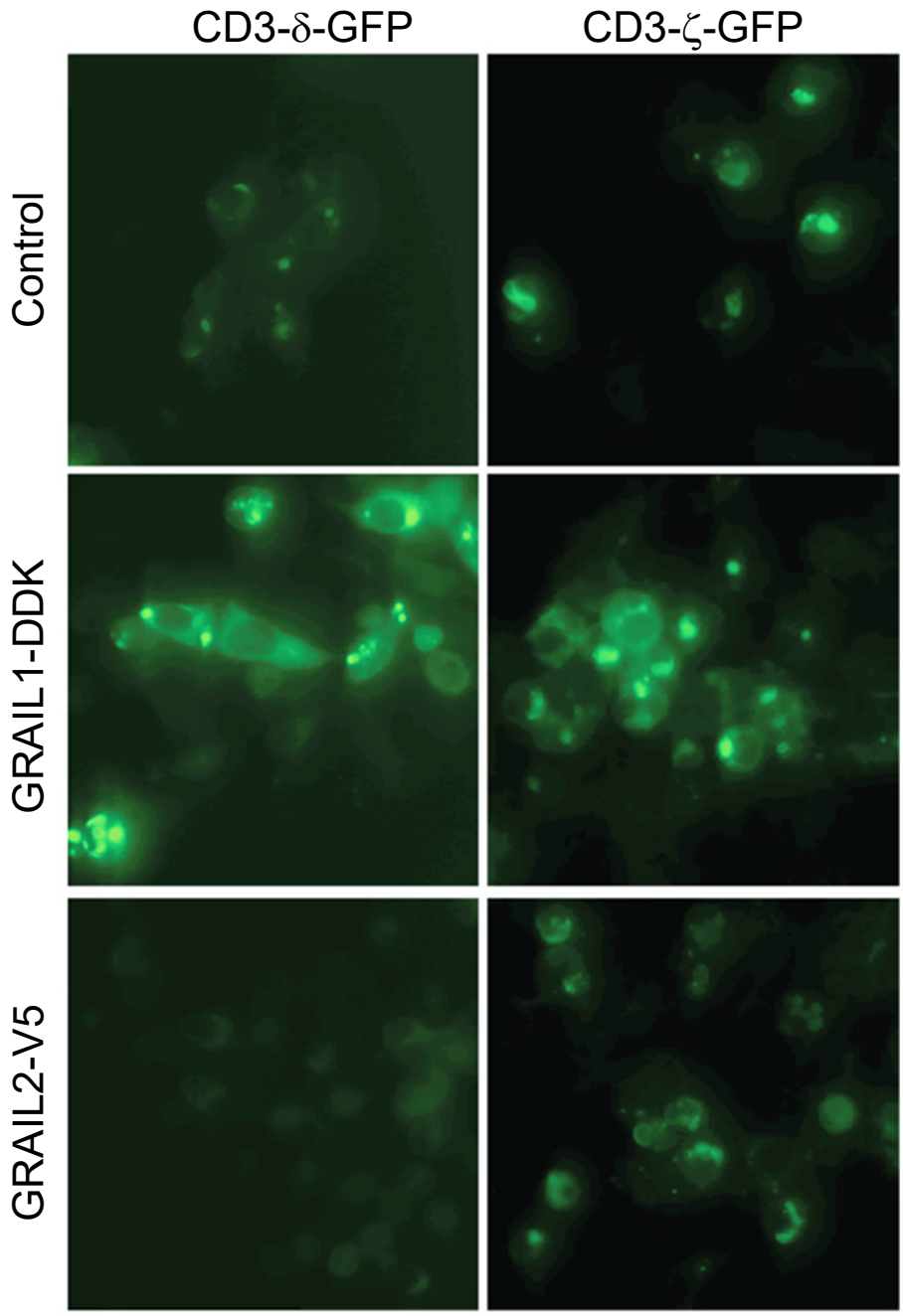

Supplemental Figure 7. Live cell imaging of HeLa cells overexpressing either GFP-tagged CD3-δ or CD3-ζ in the presence or absence of GRAIL1-DDK or GRAIL2-V5. For this study, cells were plated one day in advance followed by transfection using indicated plasmids. Images were taken 24 hours post-transfection.

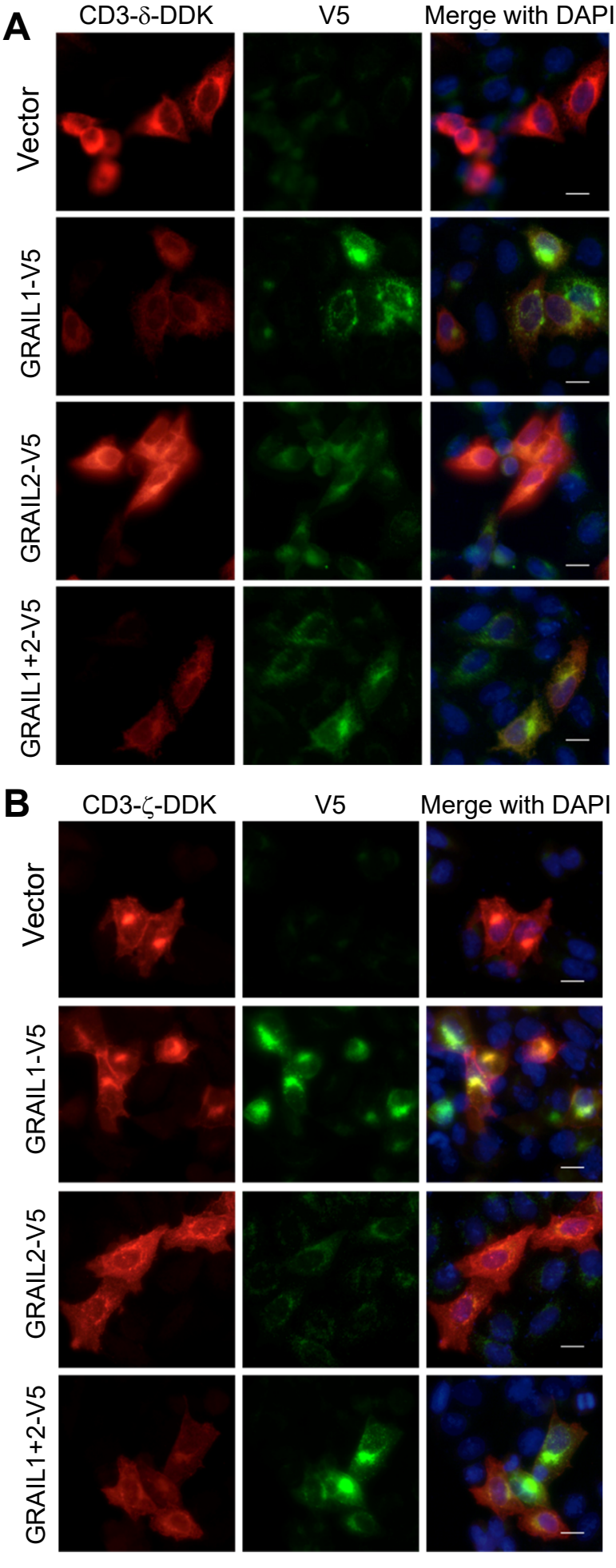

Supplemental Figure 8. Immunofluorescence (IF) staining of HeLa cells **(A)** DDK-tagged CD3-δ and **(B)** CD3-ζ in the presence and absence of either V5-tagged GRAIL1, GRAIL2, or two together as labeled. Twenty-four following transfection, cells were fixed with 10% buffered formalin and subjected to IF staining using DDK antibody (for CD3) or V5 antibody (for GRAIL). DAPI was used for nuclear staining. Scale bar, 10 μm.

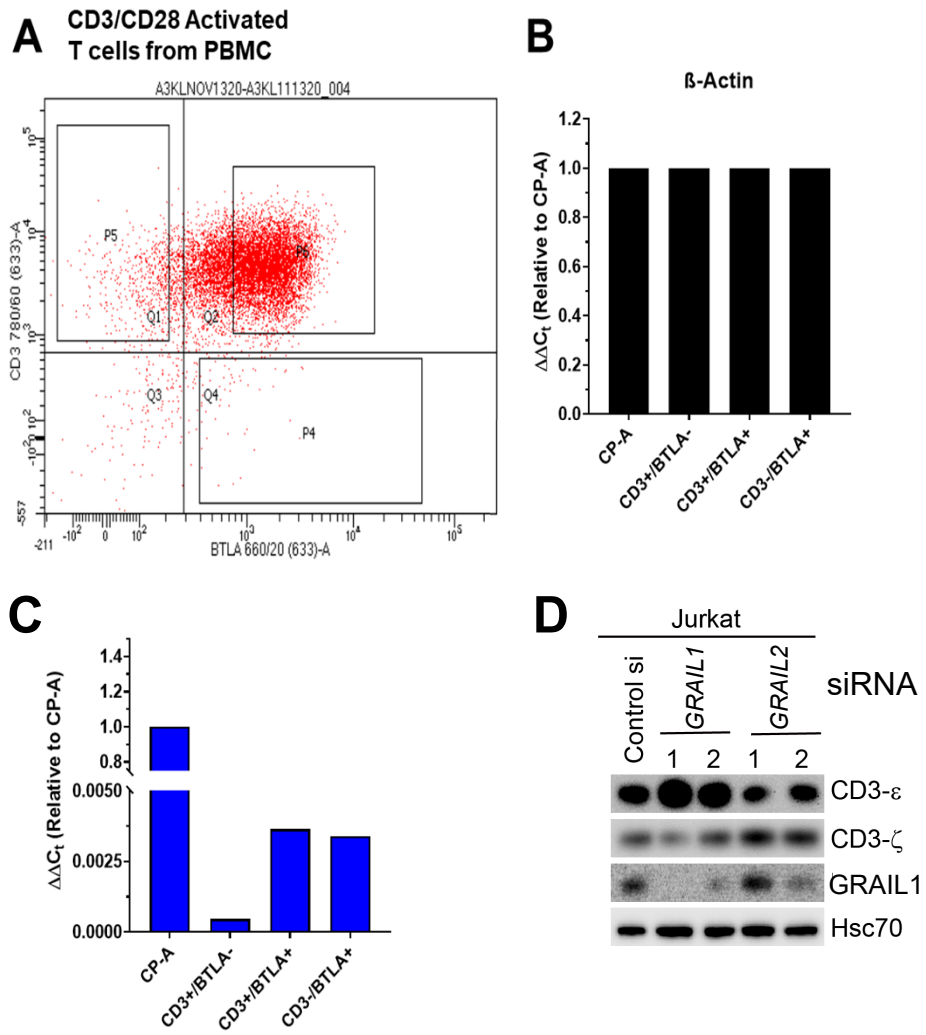

Supplemental Figure 9. Sorted T-cells from patient PBMCs were induced with αCD3-CD28 Dynabeads and were cultured for 10 days to promote T-cell exhaustion. **(A)** Cells were subjected to FACs analysis based on CD3 and BTLA expression. **(B, C)** Sorted cells as indicated were used to isolate RNAs to quantify GRAIL expression and b-actin was used as a loading control. **(D)** Jurkat cells were either transfected with control siRNA or 2 different sets of siRNA for *GRAIL1* and *GRAIL2* as indicated. Forty-eight hours post transfection, cell lysates were prepared and subjected to immunoblotting using indicated antibodies. Hsp70 was used as a loading control.

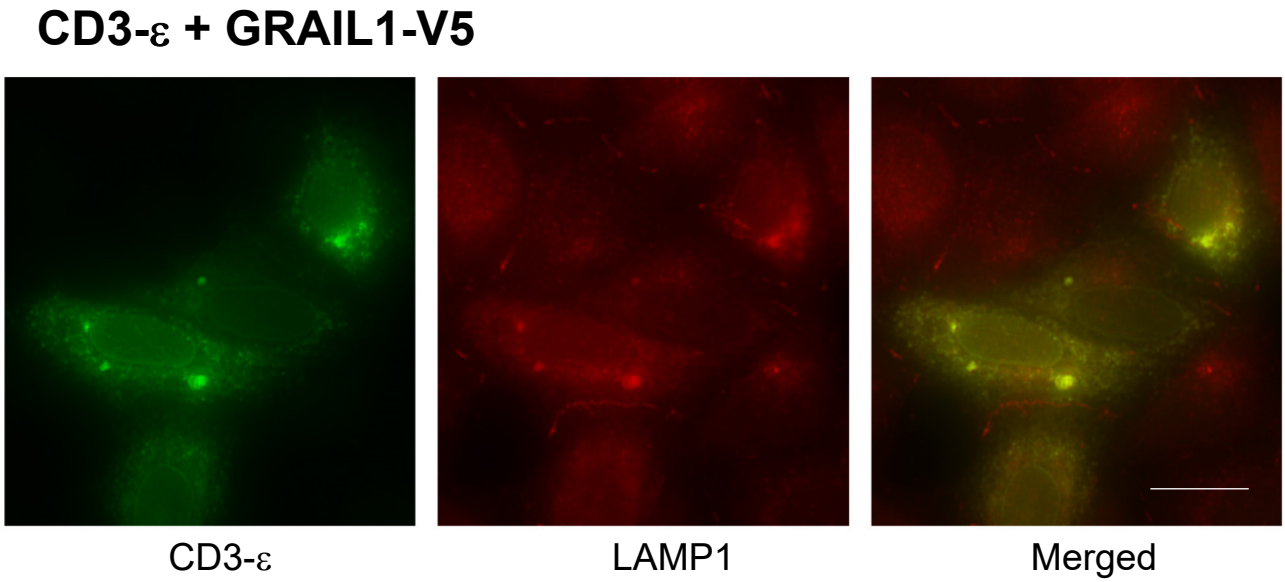

Supplemental Figure 10. DDK tagged CD3-ε when overexpressed along with V5-tagged GRAIL1, showed punctate CD3 staining. Immunofluorescence images showing CD3-ε and LAMP1 colocalization when overexpressed with GRAIL1, suggesting GRAIL mediated CD3-ε degradation is at the lysosome. Scale bar, 10 μm.

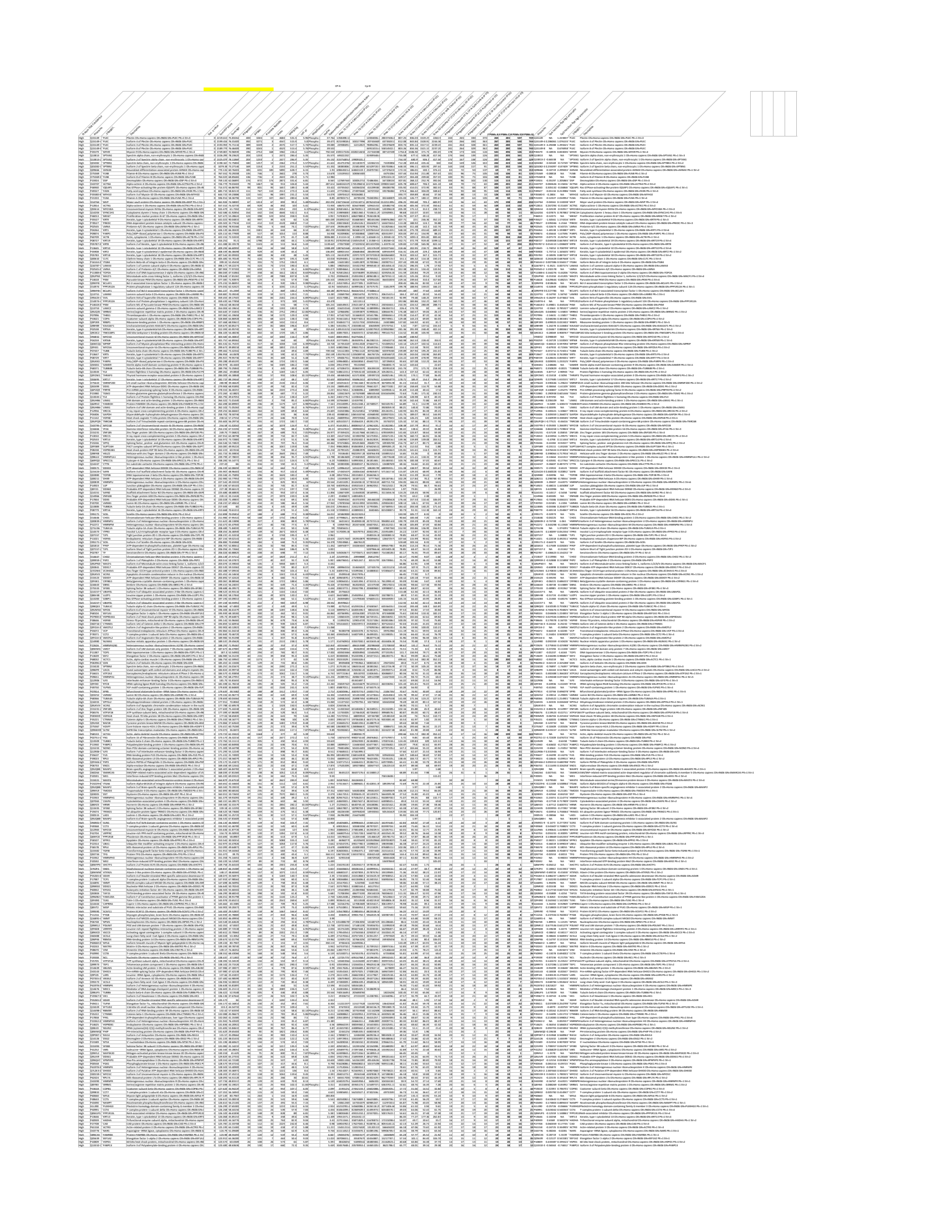

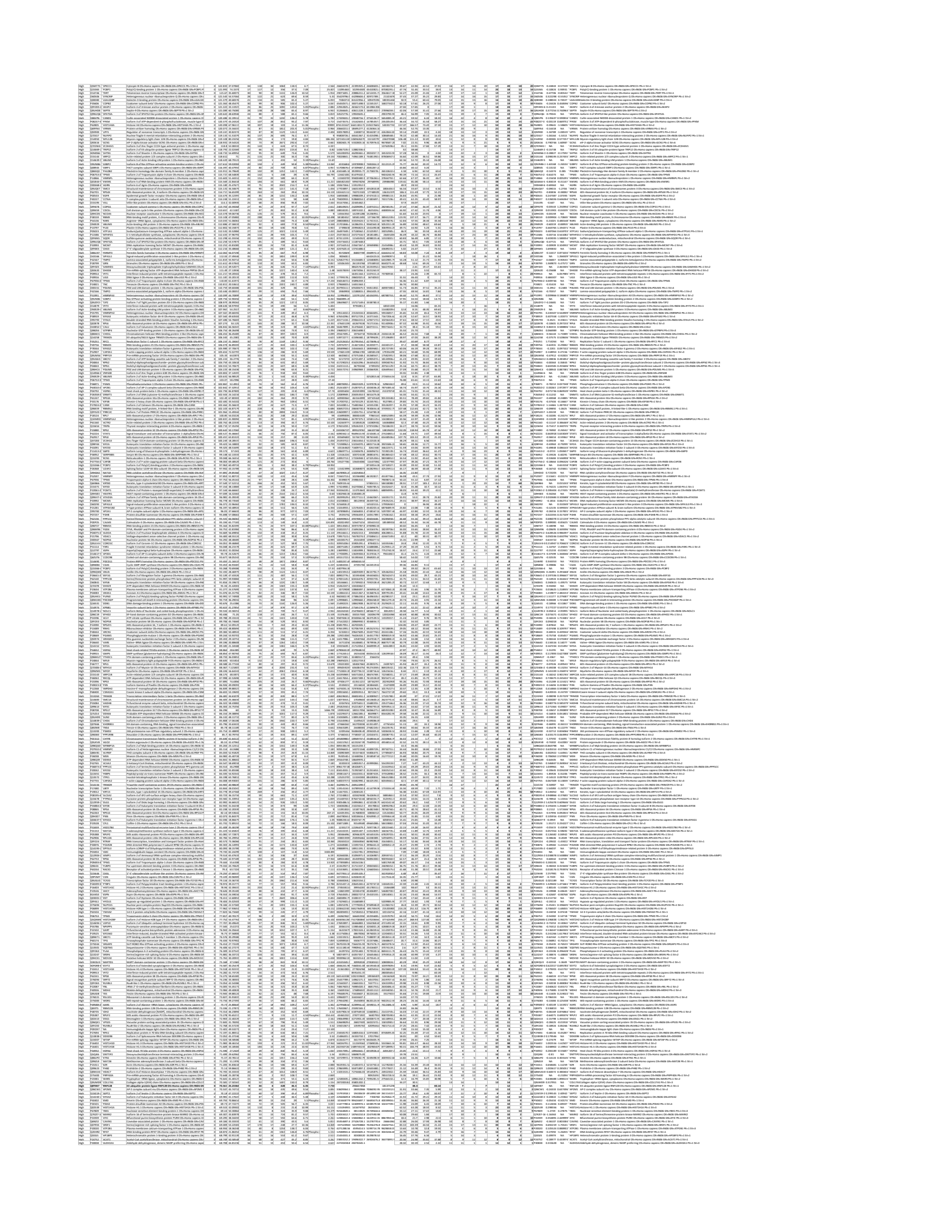

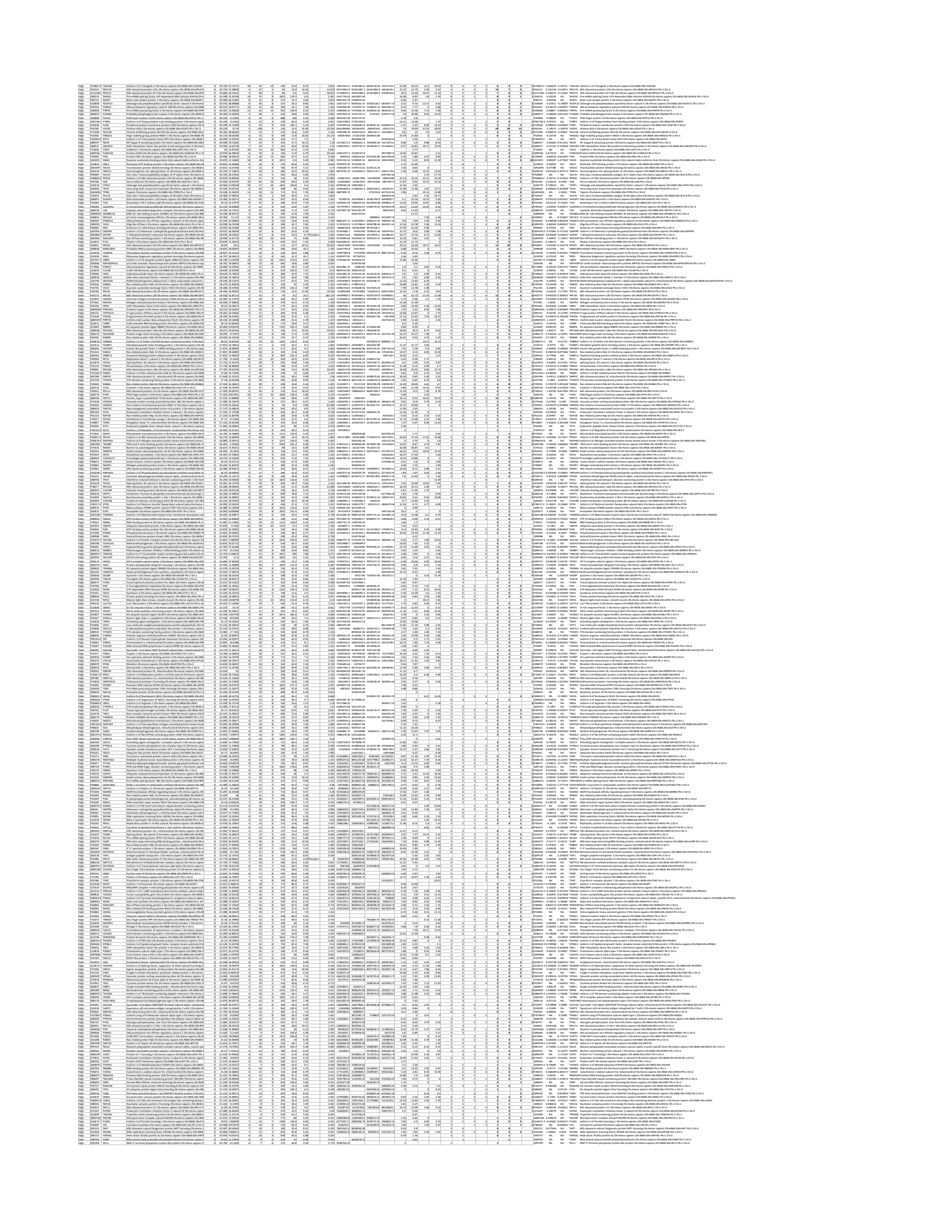

Low	C9JPN9	' USP17L12	Ubiquitin carboxyl-terminal hydrolase 17-like protein 12 OS=Homo s	0.099	1.146	6.226415	1	1	1	530	59.6	8.07		0.08	C9JPN9	NA	NA	' USP17L1	Ubiquitin carboxyl-terminal hydrolase 17-like protein 12 OS=Homo sapiens OX=9606 GN=USP17L12 PE=3 SV=1
Low	Q5TCS8	' AK9	Adenylate kinase 9 OS=Homo sapiens OX=9606 GN=AK9 PE=1 SV=2	0.101	1.119	0.994244	1	1	1	1911	221.3	5.01		0.021	Q5TCS8	NA	NA	' AK9	Adenylate kinase 9 OS=Homo sapiens OX=9606 GN=AK9 PE=1 SV=2
Low	Q92851-4	' CASP10	Isoform D of Caspase-10 OS=Homo sapiens OX=9606 GN=CASP10	0.101	1.102	3.065134	1	1	1	522	59	6.62		0.093	Q92851-4	NA	NA	' CASP10	Isoform D of Caspase-10 OS=Homo sapiens OX=9606 GN=CASP10
Low	P04430	' IGKV1-16	Immunoglobulin kappa variable 1-16 OS=Homo sapiens OX=9606 GI	0.101	1.046	13.67521	1	1	1	117	12.6	8.16		0.468	P04430	NA	NA	' IGKV1-16	Immunoglobulin kappa variable 1-16 OS=Homo sapiens OX=9606 GN=IGKV1-16 PE=1 SV=2
Low	Q9Y4H2	' IRS2	Insulin receptor substrate 2 OS=Homo sapiens OX=9606 GN=IRS2 PE	0.101	1.03	1.046338	1	1	1	1338	137.2	8.65		0.038	Q9Y4H2	NA	NA	' IRS2	Insulin receptor substrate 2 OS=Homo sapiens OX=9606 GN=IRS2 PE=1 SV=2
Low	A0A075B(	' IGLV3-16	Immunoglobulin lambda variable 3-16 OS=Homo sapiens OX=9606 (	0.101	1.013	9.565217	1	1	1	115	12.5	4.65		0.585	A0A075B6	NA	NA	' IGLV3-16	Immunoglobulin lambda variable 3-16 OS=Homo sapiens OX=9606 GN=IGLV3-16 PE=3 SV=2